Sensors and Actuators B 178 (2013) 350–358

Contents lists available at SciVerse ScienceDirect

Sensors and Actuators B: Chemical

journal homepage: www.elsevier.com/locate/snb

Final capping passivation layers for long-life microsensors in real fluids

E. Vanhove[a,b], A. Tsopéla[a,b], L. Bouscayrol[a,b], A. Desmoulin[a,b], J. Launay[a,b], P. Temple-Boyer[a,b,*]

[a] CNRS, LAAS, 7 avenue du colonel Roche, F-31400 Toulouse, France
[b] University of Toulouse, UPS, LAAS, F-31400 Toulouse, France

ARTICLE INFO

Article history:
Received 19 September 2012
Received in revised form 7 December 2012
Accepted 25 December 2012
Available online 3 January 2013

Keywords:
Passivation layer
ICP-PECVD
SiN_x films
Electrochemical microsensors

ABSTRACT

Final capping insulation layer is a critical step in the microfabrication process that determines the lifetime of analytical microsensors in real fluids. Actual processes encounter considerable limitations as (i) organic passivation layers do not provide a satisfying long-term protection against liquids and (ii) inorganic passivation processes (dielectric materials deposition and patterning) are very aggressive for the underlying layers, imposing severe constraints on the integration of sensitive materials. We present here a low temperature deposition process of high quality silicon nitride Si_3N_4 using ICP-CVD technique combined with a lift-off based process to pattern conformal deposition, in order to avoid harsh treatments such as wet or dry etching. High-density SiN_x films with low H content (5×10^{20} at/cm^3) were synthesized at 100 °C with controlled uniformity (5%), refractive index (2.025 at 830 nm), etch rate in buffered hydrofluoric acid (8 nm/min), residual stress (−500 MPa), breakdown field (3.9 MV/cm) and dielectric constant (6.0). In order to validate the compatibility of this passivation process with long-term fluids analysis, microelectrodes were fabricated and their lifetime in natural seawater was evaluated. Their active surfaces were defined by patterning the insulation layer. Special care was given to their accurate estimation through the modelling of chronoamperometric curves. Reproducible and stable electrochemical response was obtained for months (>50 days), demonstrating a considerably extended lifetime in harsh liquid media.

1. Introduction

Due to their increasing success, electrochemical microsensors are expanding upon new disciplines such as environment and biology. Embracing a very large scope of applications, they are now confronting the analysis of increasingly complex and harsh real fluids. Moreover, expected lifetime for in situ applications is constantly extended and can now reach a duration of several months. Sensors microfabrication is due to allow the integration of more and more advanced materials and complete analysis microsystems have to be produced at smaller scales. The important breakthroughs brought about by microtechnologies in terms of integration, accuracy and robustness yet enabled the exploration of new time and space scales, thus extending every day the boundaries of liquid phase analysis. A challenging issue however lays in the development of final capping passivation layers that protect the microsensors and define their active areas. Indeed, this microfabrication process key step has to meet high expectations: (i) electrical insulation, (ii) corrosion resistance and extended lifetime in liquid media, (iii) deposition and patterning processes compatible with fragile materials, (iv) precise definition of patterns and (v) chemical and biological inertness. Current passivation processes unfortunately encounter important limitations. On the one hand, patterning of inorganic dielectric layers calls for harsh etching procedures, limiting the range of materials that can be integrated. On the other hand, polymer layers cannot undergo long-term immersions in liquid. To overcome these difficulties, we propose here to combine favourable aspects of both technologies by developing (i) a low temperature deposition process of high quality silicon nitride using inductively-coupled plasma chemical vapour deposition (ICP-CVD) and (ii) a non-aggressive lift-off-based process to pattern the so-deposited conformal films. For long-term analysis in corrosive liquids, the advantages of this passivation process become much more evident through the fabrication of electrochemical microsensors for in situ marine environment monitoring and the evaluation of their lifetime in natural seawater.

2. Passivation layers study

There are nowadays two main types of materials and corresponding processes for the development of passivation layers: (i) polymers and (ii) inorganic dielectric materials.

2.1. Polymers

The polymers most commonly used as insulating coatings are epoxy resists (e.g. SU8), silicones (e.g. PDMS), poly-imides (PI), poly(p-xylene)s (e.g. parylene) and benzocyclobutenes (BCB) [1].

* Corresponding author. Tel.: +33 561 336 954.
E-mail address: temple@laas.fr (P. Temple-Boyer).

0925-4005/$ – see front matter © 2013 Elsevier B.V. All rights reserved.
http://dx.doi.org/10.1016/j.snb.2012.12.088

Table 1
Chemical, mechanical and electrical properties of a selection of widely used polymers.

	SU-8 [2–4]	PDMS [4,5]	PI [6]	Parylene [7]	BCB [8]
Density	1.075–1.153	1.08	–	1.10–1.42	–
Tensile strength (MPa)	73	6.2	260	41–76	87
Elongation at break (%)	4.8	600	100	120–250	8
Young's modulus (MPa)	2000	0.1–0.5	2300	2400–2800	2900
Residual stress (MPa)	16–19	–	18	–	28
Dielectric constant	3.28 @ 1 GHz	2.6–3.8 @ 50 Hz	3.3–3.5	2.7–3.1 @ 1 kHz	2.65 @ 1 kHz
Bulk resistivity (Ω cm)	7.8×10^{14}	10^{15}	–	$8.8–14 \times 10^{16}$	10^{19}
Breakdown field (V/cm)	$>4 \times 10^5$	2000	$>2 \times 10^6$	$5.5–7.4 \times 10^4$	5.3×10^6
Water absorption (%)	0.55 (85 RH)	<1	3.1 (85 RH)	<0.1 after 24 h	0.14 (84 RH)

A wide variety of polymers is commercially available and most of them can be deposited and patterned using microlithography techniques (soft lithography, photolithography and direct contact printing) without requiring a harsh etching process (wet etching, reactive ion etching) with the noteworthy exception of poly(p-xylene) deposited by physical vapour deposition. They thus enable the integration of fragile materials that could in any other case be irreversibly damaged by aggressive treatments, high temperatures or harsh chemical attacks.

Properties of polymer materials are presented in Table 1 [2–8]. Polymers properties are moreover largely affected by their fabrication and preparation conditions and by the resist chemical formula. The latter, which is often not communicated by the production companies, can change through different generations of products. As resists are not specifically designed for chemical analysis, the absence of interfering species has to be verified for each new formula. Last but not least, in spite of the significant advances attained, most polymers do not provide a sufficient long-term protection against liquids (i.e. several months), especially when the medium is corrosive (e.g. seawater). Thus, we observed that even the most resistant resists that are more resistant to fluids and chemical attacks (e.g. the SU-8 resist) absorb water, expand and end up cracking and delaminating from the most stressed areas (device edges). The latter leads to an irreversible deterioration of devices after only a couple of weeks spent in seawater. This short lifetime unfortunately appears as inadequate for long-term in situ measurements such as marine environment monitoring.

2.2. Inorganic dielectric materials

Inorganic dielectrics present excellent electrical barrier properties and offer a much higher protection against fluids than polymers. The most frequently used insulating materials are silicon oxide SiO_2, silicon nitride Si_3N_4 and silicon carbide SiC derivatives. More recent materials such as diamond and diamond-like carbon (DLC) have also attracted wide attention [9]. Two types of techniques are commonly employed to deposit these films, based either on chemical vapour deposition (CVD) or on physical vapour deposition (PVD). The majority of these processes takes place at high temperatures (≥300 °C) whereas just a few enable the deposition of insulating film at low temperature (≤100 °C) such as high-density plasma (HDP) and sputtering. Material properties of widely used inorganic insulating materials are displayed in Table 2 [9–49]. These properties are strongly affected by the methods, the system design and the specific recipes used to produce the films. Post-annealing can be performed to modify stress properties and chemical bonding of the deposited layers. The deposition of multi-layers was another alternative for the reduction of film stress and the enhancement of film resistance. The aforementioned processes unfortunately require a subsequent step of wet or dry etching to form patterns from blanked-deposited layers. The latter, combined with the need of high deposition temperature, is considerably limiting the range of materials that could be integrated.

Among inorganic materials, silicon nitride Si_3N_4 is a particularly attractive option for final capping passivation layers due to its high barrier properties, hydrophobicity, low porosity and high chemical resistance. These films can be obtained using various deposition techniques depending on process temperature. Typical CVD techniques require high deposition temperature (>700 °C) [9,11,16–23]. By conventional plasma-enhanced chemical vapour deposition (PECVD) [9,10,14,24–33], this temperature could be decreased down to 250–400 °C but not below 200 °C without important impact on film quality. Pulsed laser deposition [50] and catalytic CVD [51,52] are low temperature alternative processes (150 °C). Recently, major interest has been placed on the development of novel PECVD techniques for the deposition of high-density SiN_x films at low temperature with reduced surface damages and controlled residual stress. As a result, the most effective methods to produce high-quality dielectric films at low temperatures (≤100 °C) are the high-density plasma techniques such as electron cyclotron resonance plasma (ECR-CVD) [53–56] and inductively coupled plasma CVD (ICP-CVD) [57–62].

In this paper, we therefore study a low temperature ICP-CVD deposition process and a non-aggressive lift-off based patterning process to develop high quality silicon nitride Si_3N_4 films. For the validation of the so-obtained passivation process, the lifetime of electrochemical devices was evaluated in natural seawater.

3. Experimental

3.1. ICP-CVD deposition and characterization of SiN_x films

The ICP-CVD deposition system is a Plasmalab System ICP180 from Oxford Instruments Plasma Technology. The high-density plasma source of this system comprised of an inductively coupled coil connected to a 13.56 MHz, 3 kW RF generator. In the reaction chamber, the plasma generation zone is separated from the deposition zone in order to reduce damage by direct ion–surface interaction. During the deposition, the sample was clamped on the substrate electrode and an helium pressure was applied on the backside of the wafer to provide a proper thermal contact with the chuck. Feeding gases were silane SiH_4 and nitrogen N_2 (purity: 99.999%). Silane was chosen upon others less dangerous precursors (such as dichlorosilane SiH_2Cl_2 or trichlorosilane $SiHCl_3$) since it leads to higher deposition rates and chloride-free ambient. Nitrogen was preferred to ammonia NH_3 because it leads to films with lower hydrogen content. Silane was introduced in the deposition chamber through a gas distribution ring while nitrogen was introduced in the ICP source chamber. The ICP reactor is regularly cleaned using CF_4/O_2 plasma to remove any trace of contaminants and ensure process repeatability.

Thin SiN_x films (100–250 nm) were deposited on RCA-cleaned, highly doped, 4-in. silicon substrates. Deposition temperature and ICP power were fixed at 100 °C and 500 W respectively while total pressure and gas flows (silane SiH_4 and nitrogen N_2) ranged from 8 to 12 mTorr and from 10 to 25 sccm respectively. Film

Table 2
Chemical, mechanical and electrical properties of a selection of widely used inorganic materials.

	SiO_2			SiN		SiC			Diamond	
	LPCVD [9]	PECVD [9–14]	SD [9,15]	LPCVD [9,11,16–23]	PECVD [9,10,14,24–33]	LPCVD [9,34–36]	PECVD [9,27,37–40]	SD [41–43]	µCD [44–46]	UNCD, NCD [46–49]
Deposition temperature (°C)	425–700	60–400	75–285	700–900	50–400	700–1280	25–400	<170	450–850	300–800
Density				3–3.1	2.0–3.1					3.15–3.55
Expansion coefficient (ppm/°C)				2–3	1.5	4.6				
Young modulus (GPa)		53		186–412	50–242	246–530	21–180	260	710–1015	700–1050
Residual stress (MPa)	−100–200	−500 to −25	−90 to −300	−200 to 1300	−1200 to 900	−200 to 1200	−3000 to 200	−1400 to 300		−600 to 1400
Tensile strength (GPa)				5.5–6.4		3.2–23.4			0.7	0.8–5
Fracture stress (GPa)				7.1–11.7	1.52–3.27					0.9–5
Residual strain ($\times 10^3$)					−6.4 to −0.38	1–2				
Hardness (GPa)		4–8			11.2–27		8.8	10–18	30–110	55–105
Fracture toughness (MPa $\sqrt{m}$)				1.8–14	0.2–8	2.9–3				
Poisson ratio					0.25	0.21			0.07	0.07
Resistivity (Ω cm)				$\sim 10^{14}$	10^4 to 10^{20} @2 MV/cm	0.001–1000	$1–2 \times 10^7$	550	0.0001 to 10^{14}	
Breakdown field (MV/cm)				1–10	1–9				25	
Hydrogen content		3–5%		Not detected to $7 \times 10^{21} \times cm^{-3}$	10–40 at% $1–2.5 \times 10^{22} cm^{-3}$					<1–10%
Etch rate in HF (nm/min)	30–540			1	150–300 in 49% HF @ 23 °C		0.017 in 40% HF			
Etch rate in BHF (nm/min)			130–750		5–150					
Etch rate in KOH (nm/min)			3.5–5 @40 wt%	0.0022 @ pH 11	0.28–0.95 in 30% KOH @90 °C		0.022–78			
Refractive index				2.0–3.5	1.7–2.7		2.5–3.3			

thickness and refractive index were measured by ellipsometry (Uvisel Horiba Jobin Yvon) operating at a 830 nm wavelength, and were additionally verified by profilometry (KLA Tencor P16+). Etch rate was determined by wet etching at 20 °C in a buffered mixture of hydrofluoric acid (HF – 49%) and ammonium fluoride (NH_4F – 40%) with a 1:10 volume ratio. Film stress was determined by profilometry measurements of the curvature change that results from film deposition using Stoney's equation (measurement accuracy: 5%) [18]. Finally, electrical properties were characterized by current–voltage (*I–V*) and capacitance–voltage (*C–V*) experiments using a mercury probe. Thus, the breakdown voltage was measured by applying a ramped voltage across the dielectric film, and *C–V* measurements were performed at 1 KHz to determine the dielectric constant.

3.2. Microfabrication of electrochemical devices

The microfabrication process is based on the lift-off technique (use of a photoresist as a sacrificial pencil layer to pattern the blanket deposited films). Thermally oxidized (SiO_2 thickness – 600 nm) low-doped silicon substrates were used to fabricate the electrochemical microdevices. Titanium/platinum/gold layers (thickness – 12/120/120 nm) were then deposited by vacuum evaporation to form contact pads, conduction trails and working electrodes. Titanium is known to be a good adhesion promoter for metal deposition on silicon oxide, platinum is used here as a diffusion barrier and gold is the desired electroactive material. Microdevices were then passivated by depositing the SiN_x film on the whole wafer except for the electrochemical active areas (radius: 10 and 20 µm). This last patterning was performed using the lift-off technique. LOR 3A lift-off resist (Microchem) and AZ ECI 3012 photoresist (AZ Electronic Materials) were employed to form the resist pencil layers. Patterns were cleaned using Microposit MF CD-26 (Shipley) and AZ (AZ Electronic Materials) developers. Resist stripping was performed in acetone and 1:1 AZ 400K (AZ Electronic Materials)/deionised water solutions. Resist profiles, film deposits and fabricated microstructures were characterized by SEM imaging (MEB Hitachi S4800) and profilometry (see above) measurements. Finally, wafers were diced into single chips using a diamond saw. Chips were then mounted and glued on printed circuits boards. Following wire bonding, encapsulation was performed in order to conduct electrochemical measurements in liquid phase.

3.3. Electrochemical properties study

Electrochemical experiments were carried out at room temperature using a computer driven low-current potentiostat (VMP3, BioLogic) and utilizing a classical three-electrodes system. A large area of platinum-mesh, the studied microelectrode and an Ag/AgCl electrode (3 M) were used as counter, working and reference electrodes, respectively. Studies were performed in the lab while using already filtered, natural seawater. From the beginning and between each electrochemical evaluation, microdevices were immerged in a seawater-filled beaker and maintained in darkness at ambient temperature. With such procedure, no biofouling process occurs, allowing the examination of only corrosion phenomena. Prior to each set of experiments, microelectrodes were rinsed with ultrapure water and dried with pure argon gas. A typical set of measurement consisted in an electrochemical pre-treatment applied to ensure an improved repeatability by surface cleaning followed by a potential window evaluation and a chronoamperometry experiment. Electrochemical tests were repeated twice a week during more than two months (64 days). Electrochemical pre-treatments (10 scans performed between −0.4 and 1 V) and potential window evaluations (3 scans performed between −0.4 and 1.5 V) were conducted in diluted (0.5 M) solutions of sulphuric acid (96%) at

Table 3
Deposition conditions for low temperature ICP-CVD SiN_x films.

Deposition temperature	Total pressure	Silane SiH_4 flow	Nitrogen N_2 flow	ICP power	Deposition time	Deposition rate
100 °C	12 mTorr	14.5 sccm	12 sccm	500 W	18 min	7 nm/min

scan rates of 100 and 50 mV/s respectively. Chronoamperometric measurements were carried out at 0.6 V in 5 mM solutions of potassium hexacyanoferrate (II) trihydrate (Sigma–Aldrich) that were daily prepared using a 0.5 M phosphate buffer (pH 7) as supporting electrolyte. All chemicals were of at least reagent grade quality and used without additional purification.

4. Results and discussion

4.1. Deposition of ICP-CVD low temperature SiN_x films

This work is focused on the development of robust final capping passivation layers. Based on bibliographic survey, the "high-quality Si_3N_4" process provided by the Oxford Instruments Plasma Technology company and our own expertise in chemical vapour deposition, the ICP-CVD deposition parameters were examined in order to obtain a passivation layer resistant to long-term immersions into corrosive media and minimize the process-induced damages on the underlying layers.

Chemical composition (Si/N ratio and H-content) and density are the physicochemical properties that most affect the barrier properties of the SiN_x films and their resistance to corrosion [57–63]. A Si/N ratio close to 0.75 (stoichiometric silicon nitride Si_3N_4) and a high density thus favour strong resistance to chemical attack (high bond strength, minimization of the dandling bonds). On the contrary, high hydrogen content, high pinhole defect density and/or high porosity strongly degrade the film chemical and electrical properties and can engender a poor long-term stability due to hydrogen atoms out-diffusion. Concentrations of active species (active nitrogen and SiH_x precursors) at the sample surface are the key process factors that determine the film composition and structure. These two factors can be controlled by adjusting the ICP power, the total pressure and the SiH_4/N_2 gas flow ratio.

Since the ICP source can easily dissociate the reactant gases, effect of substrate temperature is lower than effects of ICP power, chamber pressure and gas flows [62]. Reducing deposition temperature brings about much more versatility in the microfabrication processes and ensures technological compatibility with photoresist layers used to pattern the deposited SiN_x films. Nevertheless, the lower this temperature, the more difficult it is to obtain high quality films [60,62]. Indeed, substrate temperature, by favouring hydrogen release from the surface, has an impact on film properties, i.e. film density, hydrogen content and amorphous silicon incorporation. A deposition temperature of 100 °C was therefore chosen in order to avoid the deterioration of underlying layers while not degrading the quality of the film.

The ICP power affects the dissociation rate of feeding gases and, consequently, the concentration of active species and the deposition rate [57,58,61]. As nitrogen N_2 dissociation requires more energy than silane SiH_4 dissociation, it also impacts the active species gaseous ratio [57,63]. An increase in ICP power thus results in a higher deposition rate and an increase in the film N/Si ratio. According to Xu [59], such an increase is also encouraging the formation of stable Si—N bonds and higher quality films as it reduces the film hydrogen content. Increasing ICP power may also generate a higher surface sputtering [59], even if the ICP-CVD technique drastically reduces the surface damage induced by ion bombardment [62].

An increase in total pressure brings about an increase in the concentration of active species and therefore in the deposition rate [57,61]. It also leads to a higher N/Si ratio [57,62,63]. Reducing the deposition rate tends to improve film quality [57], probably by providing sufficient time for hydrogen to outgas from the growing film [61] or atoms to reach the lowest energy state [57]. The growth of dense films is moreover slower compared to the growth of porous ones. An alternative to increase deposition rate while maintaining high film quality could be to increase ICP power and gas flow mixture, as suggested by Owain [61].

ICP power, total pressure and SiH_4 ratio were thus adjusted to control the ratio of Si/N around 0.75 and decrease the hydrogen content and defect density while obtaining a slow but reasonable deposition rate. Finally, the film thickness, and consequently the deposition time, were chosen to provide excellent electrical insulation and chemical resistance in liquid media while limiting any negative effect related to the film residual stress. Indeed, the ICP-CVD deposition of stoichiometric silicon nitride Si_3N_4 leads to a highly compressive stress [57]. Although high stress has no direct impact on the electrochemical performances, it can strongly hamper the microfabrication processes and be responsible for a more rapid corrosion if microcracks are formed at the microdevice edges. Owing to the excellent barrier properties of ICP-CVD SiN_x films, it is possible to lower the film thickness to 100 nm. It moreover allows to decrease the microelectrode recess. Optimized ICP-CVD deposition parameters for the deposition of silicon nitride as passivation layer are summarized in Table 3.

4.2. Characterization of ICP-CVD SiN_x films deposited at low temperature

The characteristics of the optimized ICP-CVD SiN_x films are presented in Table 4 and discussed in the following paragraphs. Film thickness was determined by ellipsometry and verified by profilometry. Deposition rate, estimated at 7 nm/min, was reproducible. This rate, slightly lower than typical results obtained for ICP-CVD (>8 nm/min) [61], leads to high-quality SiN_x films (see above). Thickness uniformity across 4-inch wafers was estimated at 5%, close to 3% reported by Owain [61], and indicates a uniform deposition.

The refractive index, estimated around 2.025 at a 830 nm wavelength, is representative of the chemical composition of the SiN_x films [57,61,62] but does not allow the determination of simultaneously the Si/N ratio and hydrogen content. In order to do so, the film refractive index was measured after a dehydrogenation thermal annealing (600 °C – 2 h). A value around 2.05 was obtained and the Si/N ratio was finally calculated to be 0.8 by applying the Bruggeman theory to the Si/Si_3N_4 heterogeneous medium [64].

Table 4
Characteristics of the optimized ICP-CVD SiN_x films.

Stoichiometry	Thickness	Refractive index (830 nm)	BHF etch rate	Residual stress	Breakdown field	Dielectric constant
$SiN_{1.25}H_{0.01}$	125 ± 6 nm	2.025	8 nm/min	−500 ± 25 MPa	>3.9 MV/cm	6.0 ± 0.1

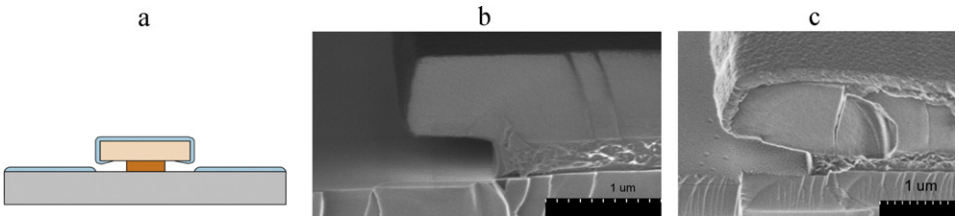

Fig. 1. Silicon nitride deposition on T-shaped bilayer resist (a), SEM images of the T-shaped bilayer resist profile (b) before and (c) after the SiN_x film deposition.

Given the Si/N ratio, the hydrogen content was finally obtained from the as-deposited film refractive index by applying the Bruggeman theory to the $Si/Si_3N_4/H_2$ heterogeneous medium. Hence, it was estimated at approximately 4×10^{20} at/cm^3, i.e. lower than 1%. This low value is in agreement with the hydrogen content measured by Zhou et al. (from 1 to 3% depending on film depth) [62] and is much lower than values obtained by Da Silva Zambon et al. ($\sim 10^{21}$ at/cm^3) [58] and Han et al. (from 3 to 6×10^{21} at/cm^3) [63].

Film quality is also demonstrated after carrying out wet etching procedure [57,61]. The film resistance to chemical etching depends on both film density and composition. The etching rate of ICP-CVD SiN_x films at room temperature in buffered hydrofluoric acid (BHF, volume ratio 10:1) was estimated at 8 nm/min. This rate is lower than those measured by Owain (20 nm/min in 10:1 BHF) [61] and Jatta et al. (20 nm/min in 7:1 BHF) [57].

Deposited SiN_x films present a highly compressive residual stress (-500 ± 25 MPa). Such a high stress is expected as Jatta et al. demonstrated a correlation between high residual stress, low etch rate and high density [57]. They attributed such a high compressive stress to low hydrogen content. Thus, the obtained residual stress is coherent with previous results and is a positive aspect for its future performances as passivation layer. This was confirmed through electrical characterization. A breakdown electric field higher than 3.9 MV/cm was evidenced by I–V measurements. This value is very close to the one reported by Zhou et al. (>4 MV/cm) [62] and slightly higher than the one measured by Owain et al. (>3 MV/cm) [61]. Finally, dielectric properties of SiN_x films were determined by C–V measurements at 1 MHz (capacitor area: 4.18×10^{-3} cm^2). The dielectric constant was estimated at 6.0 ± 0.1. Such values are in agreement with those obtained for SiN dielectrics deposited by PECVD (dielectric constant from 6 to 8 [10]). They are representative of high-quality ICP-CVD SiN_x films and suggest that a further decrease in thickness (lower than 100 nm) is still possible.

4.3. SiN_x film micropatterning

After optimizing the parameters for the deposition of high quality, SiN_x passivation layers at low temperature (100 °C), the patterning of these layers through lift-off process has to be studied. The development of a photolithography process to pattern final capping layers needs to reach two contradictory requirements: (i) a conformal deposition allowing a perfect step coverage in order to avoid possible leakage currents, (ii) the necessity to create discontinuities in the SiN_x deposited film so that the solvents can reach and remove the sacrificial photoresist. A bilayer photolithographic process combining two photoresist layers was thus developed to overcome this difficulty through the development of T-shaped resist profiles (Fig. 1a). In order to avoid the SiN_x deposition under the T cap, the ratio "recess depth/T-shape base height" was optimized by adjusting process parameters (Table 5). Fig. 1b and c present SEM images of the cross section of T-shaped resist profiles before and after ICP-CVD process. It can be seen that T-shaped resist patterns were not damaged during deposition. Conformity of the SiN_x deposited film is estimated at approximately 1. Finally, the effectiveness of the lift-off process was assessed. 92% of the wafer structures were successfully released, demonstrating the process reliability.

4.4. Electrochemical microsensors fabrication and characterization

The aforementioned deposition and patterning processes were applied to the development of electrochemical microsensors. Microfabrication process was optimized with the objective to extend device lifetime. As previously stated, SiN_x film thickness was reduced to ~120 nm in order to avoid any stress-related defects. The Ti/Pt/Au step height was also lowered as much as possible (~250 nm since minimum height was required to perform bonding). As the SiN_x film had the tendency to delaminate on gold surfaces, silicon nitride adhesion on the gold upper layer was improved by performing just before deposition an ammonia/nitrogen plasma treatment to clean sample surface. This pre-treatment creates an hydrogenated surface that enhances film adhesion and electrical properties. Cleaning treatment was however found to possibly damage photoresist profiles. Its duration was therefore minimized to 30 s to provide the best cleaning without damaging the photoresist. The complete microfabrication process was finally validated and the obtained microelectrode is displayed in Fig. 2 (microscope and SEM images).

Microelectrode geometry has to reach high requirements: active surfaces have to be defined with a high accuracy as the measurement is directly proportional to their areas. Microelectrodes must also have a low recess depth and smoothed edges so that diffusion can correctly be described by the inlaid microdisk theory.

Table 5
Bilayer photolithography process parameters.

Layer	#1	#2
Photoresist	LOR 3A	AZ ECI 3012
Thickness	0.25 μm	1.2 μm
Softbake	170 °C, 120 s	90 °C, 60 s
UV exposure	H line, 100 mJ/cm^2	
Post exposure bake	110 °C, 60 s	
Developer	MCD26, 10 s	AZ developer 1:1, 30 s
Bake	105 °C, 60 s	
Developer	MCD26, 75 s	
Stripping	Acetone, 5 min with ultrasounds	AZ 400K, 5 min with ultrasounds

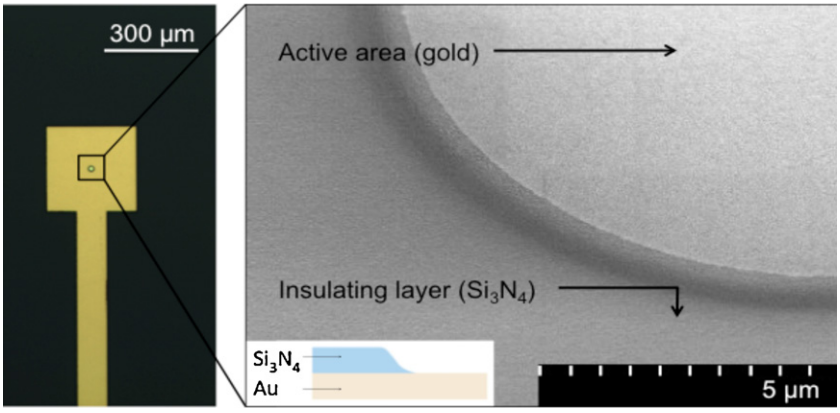

Fig. 2. Microscope image and (insert) SEM image of a typical gold microelectrode.

Microelectrode radius standard deviation was estimated at around 1% from microscope images, which corresponds to measurement accuracy. Resist pattern recess depth was controlled to obtain smooth electrode recess edges.

Electrochemical performances of obtained microdevices were finally characterized. Microfabricated devices should exhibit electrochemical behaviour similar to the one of individually produced microelectrodes. More particularly, "thin film" materials need to present electrochemical features identical to solid materials and passivation layer should prevent any leakage current flow or interfering current flow derived from underlying layers. The quality of electroactive and insulating materials was therefore assessed by cyclic voltammetry in a diluted solution of sulphuric acid. These tests were systematically repeated on several microelectrodes. An electrochemical behaviour identical to the one of solid gold was thus demonstrated with low background currents and no interfering signals (Fig. 3).

A special emphasis was placed on the evaluation of electrochemically active areas as they have a direct impact on the accuracy of the electrochemical detection. Electrochemically active area can significantly differ from geometrical area as surface asperities and roughness can lead to a microscopic area much more extended than the projected area. They can be determined by chronoamperometry from the steady state current recorded when a potential is applied. Simulation of the chronoamperometric curves presents two important advantages. Firstly, the electrochemically active area can be precisely estimated. Secondly, two out of three variables taking part in the equations can be determined while the third one is a data. These data are the radius of the electroactive area, the diffusion coefficient and the concentration of the electroactive species. For this determination, the evolution of diffusion laws, from linear diffusion at short time scales to hemispherical diffusion at long time scales is taken into account. Each curve was therefore simulated using models based on the equation developed by Aoki and Osteryoung for $\tau > 1$ (Eq. (1)) [65]:

$$I = 4nFDC^{sol}r(1 + 0.71835\tau^{-1/2} + 0.05626\tau^{-3/2} - 0.00646\tau^{-5/2}) \quad (1)$$

where I is the current intensity, n is the number of electrons involved in the electrochemical reaction, F is the Faraday constant, D and C^{sol} are the diffusion coefficient and the bulk concentration of the reduced species respectively, r is the microelectrode radius and τ is a dimensionless variable equal to $4Dt/r^2$, t being the time.

Only the two first terms of Eq. (1) were taken into account. It was numerically verified that the discarded terms represented less than 1/1000 of the current intensity. The simplified equation written for each data point forms a linear system that was resolved by the method of least squares. This model was used to monitor the evolution of the microelectrode electroactive area, the ferrocyanide concentration being experimentally known and the diffusion coefficient determination being used to check the model likelihood (situation reversed to detection).

As electrochemical microdevices were designed to perform series of electrochemical measurements in marine environment over a period of several months, their long-term response was tested. Twelve microelectrodes (radius: 10 and 20 µm) were immersed in natural seawater for 64 days. Each microelectrode was characterized twice a week by voltammetry and chronoamperometry. The evolution through time of microelectrode properties and more particularly of the electroactive area radius was studied. A lifetime higher than 50 days was recorded for all monitored microelectrodes (Fig. 4). Experimental and theoretical curves perfectly coincide whatever the microelectrode radius (Fig. 5). Estimated radius values confirm the area measurements verified by microscope images (Fig. 6). Hexacyanoferrate ion $Fe(CN_6)^{4-}$ diffusion

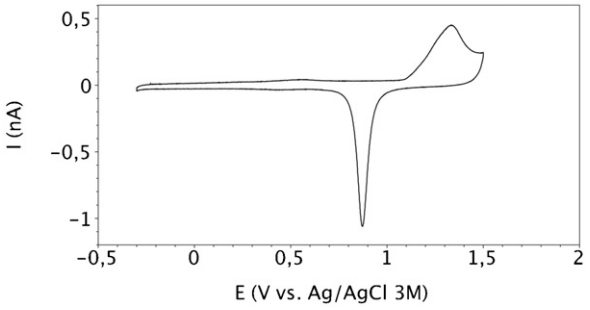

Fig. 3. Gold microelectrode ($r = 10$ µm) cyclic voltammogram. in a deaerated 0.5 M H_2SO_4 solution (potential scan rate: 50 mV/s).

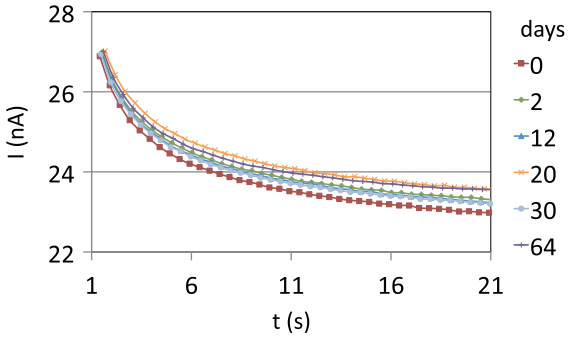

Fig. 4. Temporal evolution of chronoamperometric curves. ($[Fe(CN)_6^{4-}] = 5$ mM, $E = 0.6$ V vs Ag/AgCl) during ageing in natural seawater ($r = 20$ µm).

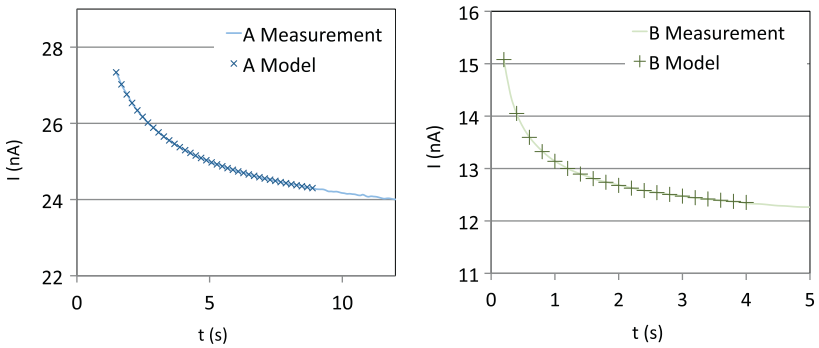

Fig. 5. Chronoamperometric curves in seawater ($[Fe(CN)_6^{4-}]$ = 5 mM, E = 0.6 V vs Ag/AgCl: experimental data (+) and simulation (line) – left: r = 20 μm, right: r = 10 μm.

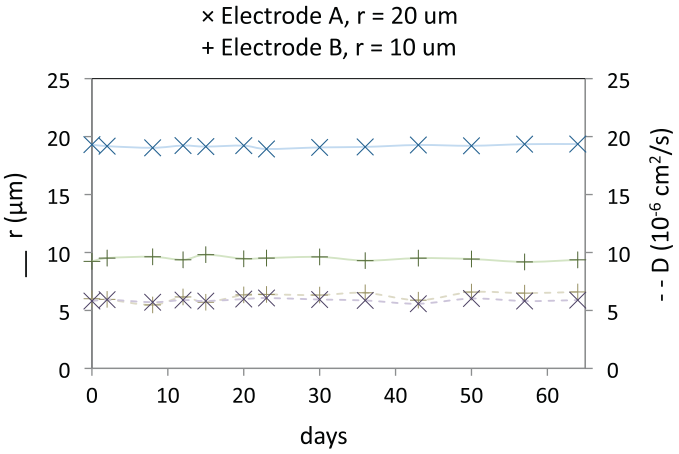

Fig. 6. Temporal evolution of microelectrode electroactive surface radius r and of $Fe(CN_6)^{4-}$ diffusion coefficient D test values during ageing in natural seawater.

coefficient values resulting from the simulation are consistent with values reported in literature [66] (Fig. 6). Electroactive surface areas were reproducible and remain stable ($\sigma_{radius=10\,\mu m}$ = 2.17%, $\sigma_{radius=20\,\mu m}$ = 2.06%) through the device lifetime. These results validate the reproducibility and the robustness of the microfabricated devices.

5. Conclusion

High quality $SiN_{1.25}H_{0.01}$ thin films (thickness: ~120 nm, refractive index at a 830 nm wavelength: 2.025, uniformity 5%) were deposited by ICP-CVD at low temperature (100 °C). The obtained layers present very good insulating properties (breakdown voltage: >3.9 MV/cm^2, dielectric constant: 6.0 ± 0.1), excellent moisture and diffusion barrier properties, hydrophobicity and high resistance to chemical attack (etch rate: 8 nm/min in a 10:1 BHF solution). ICP-CVD SiN_x films can therefore be considered as a final capping insulating layer for electrochemical microsensors and more widely MEMS applications.

The low deposition temperature not only allows the integration of temperature–sensitive materials but also makes the deposition process compatible with photoresists commonly used in microtechnologies. Thus, a patterning process which was non-aggressive for the underlying layers was developed. Due to this process, based on the development of T-shaped photoresist profiles, lift-off technique can be performed, in spite of the perfectly conformal deposition. Therefore, an enlargement of the range of materials that can be included in MEMS microdevices and a higher versatility of microfabrication processes are attained.

To validate their advantages for microsensors protection in liquid and corrosive media, the deposition and patterning processes were then applied for the development of electrochemical microsensors. As the degradation of the passivating layer would lead to an increase in the electrode active area and the emergence of interfering electrochemical signals, emphasis was placed on the accurate evaluation of the electroactive area as a function of the immersion duration in corrosive media. A model based on the Aoki and Osteryoung equation was therefore developed to analyze the obtained amperometric curves and give way to high precision estimation of the active area. Microelectrodes lifetime in natural seawater was finally assessed on a representative number of microelectrodes through periodic electrochemical measurements (cyclic voltammetry and chronoamperometry). Electrochemical areas were found to be stable and reproducible ($\sigma_{r=10\,\mu m}$ = 2.17%, $\sigma_{r=20\,\mu m}$ = 2.06%) through the device lifetime (>50 days). Owing to these very good results, ICP-CVD SiN_x was found to be an excellent candidate for MEMS passivation and protection especially for applications including long-term measurements in corrosive liquid media.

Acknowledgements

Fabricated devices will be applied for the detection of silicates in synthetic media and natural seawater through a collaboration with the LEGOS (Laboratoire d'Etudes en Géophysique et Océanographie Spatiales) in the framework of the French project MAISOE (Microlaboratoires d'Analyse In Situ pour des Observatoires Environnementaux). The authors would like to thank the French RTRA STAE (Réseau Thématique de Recherche Avancée "Sciences et Technologies pour l'Aéronautique et l'Espace") for financial support.

References

[1] E. Meng, X. Zhang, W. Benard, Additive processes for polymeric materials, in: R. Ghodssi, P. Lin (Eds.), MEMS Materials and Processes Handbook, Springer, Boston, MA, 2011, pp. 193–271.
[2] Material Data Sheet SU8_3000 version 2006, Microchem Corp., Newton, USA, s.d.
[3] H. Lorenz, M. Laudon, P. Renaud, Mechanical characterization of a new high-aspect-ratio near UV-photoresist, Microelectronic Engineering 41–42 (1998) 371–374.
[4] C. Hassler, T. Boretius, T. Stieglitz, Polymers for neural implants, Journal of Polymer Science B 49 (2011) 18–33.
[5] Material Data Sheet MED_1000 and MED_1011, version 2010, Nusil Technology LLC, Carpinteria, USA, s.d.
[6] Material Data Sheet PI_2545 version 2009, HD MicroSystems, Parlin, USA, s.d.
[7] Material Data Sheet Parylene version 2005, Specialty Coating Systems, Indiana, USA, s.d.
[8] Material Data Sheet Cyclotene_4000 version 2005, The Dow Chemical Company, s.d.
[9] C.A. Zorman, R.C. Roberts, L. Chen, Additive Processes for Semiconductors and Dielectric Materials, Springer, New York, 2011.
[10] G. Schmitt, J.W. Schultze, F. Faßbender, G. Buß, H. Lüth, M.J. Schöning, Passivation and corrosion of microelectrode arrays, Electrochimica Acta 44 (1999) 3865–3883.

[11] J. Laconte, F. Iker, S. Jorez, N. André, J. Proost, T. Pardoen, D. Flandre, J.P. Raskin, Thin films stress extraction using micromachined structures and wafer curvature measurements, Microelectronic Engineering 76 (2004) 219–226.
[12] X. Zhang, K.S. Chen, R. Ghodssi, A.A. Ayón, S.M. Spearing, Residual stress and fracture in thick tetraethylorthosilicate (TEOS) and silane-based PECVD oxide films, Sensors and Actuators A 91 (2001) 373–380.
[13] A. Tarraf, J. Daleiden, S. Irmer, D. Prasai, H. Hillmer, Stress investigation of PECVD dielectric layers for advanced optical MEMS, Journal of Micromechanics and Microengineering 14 (2004) 317–323.
[14] G. Subhash, P. Hittepole, S. Maiti, Mechanical properties of PECVD thin ceramic films, Journal of the European Ceramic Society 30 (2010) 689–697.
[15] V. Bhatt, S. Chandra, Silicon dioxide films by RF sputtering for microelectronic and MEMS applications, Journal of Micromechanics and Microengineering 17 (2007) 1066–1077.
[16] J. Gardeniers, H. Tilmans, C. Visser, LPCVD silicon-rich silicon nitride films for applications in micromechanics, studied with statistical experimental design, Journal of Vacuum Science and Technology A 14 (1996) 2879–2892.
[17] J. Yang, J. Gaspar, O. Paul, Fracture properties of LPCVD silicon nitride and thermally grown silicon oxide thin films from the load-deflection of long Si_3N_4 and SiO_2/Si_3N_4 diaphragms, Journal of Microelectromechanical Systems 17 (2008) 1120–1134.
[18] P. Temple-Boyer, C. Rossi, E. Saint-Etienne, E. Scheid, Residual stress in low pressure chemical vapor deposition SiN_x films deposited from silane and ammonia, Journal of Vacuum Science and Technology A 16 (1998) 2003–2007.
[19] A. Kaushik, H. Kahn, A. Heuer, Wafer-level mechanical characterization of silicon nitride MEMS, Journal of Microelectromechanical Systems 14 (2005) 359–367.
[20] C.H. Mastrangelo, Y.C. Tai, R.S. Muller, Thermophysical properties of low-residual stress silicon-rich LPCVD silicon nitride films, Sensors and Actuators A 23 (1990) 856–860.
[21] L.S. Fan, R.T. Howe, R.S. Muller, Fracture toughness characterization of brittle thin films, Sensors and Actuators A 23 (1990) 872–874.
[22] R.M. Tiggelaar, A.W. Groenland, R.G.P. Sanders, J.G.E. Gardeniers, Electrical properties of low pressure chemical vapor deposited silicon nitride thin films for temperatures up to 650 °C, Journal of Applied Physics 105 (2009), 1-6, 033714.
[23] G.F. Eriksen, K. Dyrbye, Protective coatings in harsh environments, Journal of Micromechanics and Microengineering 6 (1996) 55–57.
[24] E. Herth, B. Legrand, L. Buchaillot, N. Rolland, T. Lasri, Optimization of SiN_x:H films deposited by PECVD for reliability of electronic, microsystems and optical applications, Microelectronic Reliability 50 (2010) 1103–1106.
[25] S. King, R. Chu, G. Xu, J. Huening, Intrinsic stress effect on fracture toughness of plasma enhanced chemical vapor deposited SiN_x:H films, Thin Solid Films 518 (2010) 4898–4907.
[26] P.H. Wu, I.K. Lin, H.Y. Yan, K.S. Ou, K.S. Chen, X. Zhang, Mechanical property characterization of sputtered and plasma enhanced chemical deposition (PECVD) silicon nitride films after rapid thermal annealing, Sensors and Actuators A 168 (2011) 117–126.
[27] C. Iliescu, M. Avram, B. Chen, A. Popescu, V. Dumitrescu, D.P. Poenar, A. Sterian, D. Vrtacnik, S. Amon, P. Sterian, Residual stress in thin films PECVD depositions: a review, Journal of Optoelectronic and Advanced Materials 13 (2011) 387–394.
[28] J. Gaspar, M.E. Schmidt, J. Held, O. Paul, Wafer-scale microtensile testing of thin films, Journal of Microelectromechanical Systems 18 (2009) 1062–1076.
[29] H.U. Rahman, A. Gentle, E. Gauja, R. Ramer, Characterisation of dielectric properties of PECVD silicon nitride for RF MEMS using reflectance measurements, in: Proceedings of the 12th IEEE International Conference, New York, 2008.
[30] M. Jo, S. Park, S. Park, A study on resistance of PECVD silicon nitride thin film to thermal stress-induced cracking, Applied Surface Science 140 (1999) 12–18.
[31] C. Iliescu, F. Tay, J. Wei, Low stress PECVD-SiN_x layers at high deposition rates using high power and high frequency for MEMS applications, Journal of Micromechanics and Microengineering 16 (2006) 869–874.
[32] H. Huang, K.J. Winchester, A. Suvorova, B.R. Lawn, Y. Liu, X.Z. Hu, J.M. Dell, L. Faraone, Effect of deposition conditions on mechanical properties of low-temperature PECVD silicon nitride films, Material Science and Engineering A 435 (2006) 453–459.
[33] W. Zhou, J. Yang, Y. Li, A. Ji, F. Yang, Y. Yu, Bulge testing and fracture properties of plasma-enhanced chemical vapour deposited silicon nitride thin films, Thin Solid Films 517 (2009) 1989–1994.
[34] X. Fu, R. Jezeski, C. Zorman, M. Mehregany, Use of deposition pressure to control residual stress in polycrystalline SiC films, Applied Physics Letters 84 (2004) 341–343.
[35] D. Choi, R.J. Shinavski, W.S. Steffier, S.M. Spearing, Residual stress in thick low-pressure chemical-vapor deposited polycrystalline SiC coatings on Si substrates, Journal of Applied Physics 97 (2005) 1–9, 074904.
[36] X.A. Fu, J.L. Dunning, M. Mehregany, C.A. Zorman, Low stress polycrystalline SiC thin films suitable for MEMS applications, Journal of the Electrochemical Society 158 (2011) H675–H680.
[37] A. Klumpp, U. Schaber, H.L. Offereins, K. Kühl, H. Sandmaier, Amorphous silicon carbide and its application in silicon micromachining, Sensors and Actuators A 41 (1994) 310–316.
[38] H. Zhang, H. Guo, Y. Wang, G. Zhang, Z. Li, Study on a PECVD SiC-coated pressure sensor, Journal of Micromechanics and Microengineering 17 (2007) 426–431.
[39] P. Sarro, C. de Boer, E. Korkmaz, J. Laros, Low-stress PECVD SiC thin films for IC-compatible microstructures, Sensors and Actuator A 67 (1998) 175–180.
[40] W. Daves, A. Krauss, N. Behnel, V. Haeublein, A. Bauer, L. Frey, Amorphous silicon carbide thin films (a-SiC:H) deposited by plasma-enhanced chemical vapor deposition as protective coatings for harsh environment applications, Thin Solid Films 519 (2011) 5892–5898.
[41] F. Nabki, T.A. Dusatko, S. Vengallatore, M.N. El-Gamal, Low-stress CMOS-compatible silicon carbide surface-micromachining technology.Part I: process development and characterization, Journal of Microelectromechanical Systems 20 (2011) 720–729.
[42] N. Ledermann, J. Baborowski, P. Muralt, N. Xantopoulos, J. Tellenbach, Sputtered silicon carbide thin films as protective coating for MEMS applications, Surface and Coatings Technology 125 (2000) 246–250.
[43] S. Inoue, T. Namazu, H. Tawa, M. Niibe, K. Koterazawa, Stress control of a-SiC films deposited by dual source DC magnetron sputtering, Vacuum 80 (2006) 744–747.
[44] W. Gajewski, P. Achatz, O.A. Williams, K. Haenen, E. Bustarret, M. Stutzmann, J.A. Garrido, Electronic and optical properties of boron-doped nanocrystalline diamond films, Physical Review B 79 (2009) 1–14, 045206.
[45] M.C. Christopher, J.L. Davidson, L. Jiang, W.P. Kang, J.J. Sheehy, R.L. Steinbach, Diamond film as an FET gate dielectric material: diamond materials VI, The electrochemical Society (2000) 354–359.
[46] D.K. Reinhard, T.A. Grotjohn, M. Becker, M.K. Yaran, T. Schuelke, J. Asmussen, Fabrication and properties of ultrananno, nano, and microcrystalline diamond membranes and sheets, Journal of Vacuum Science and Technology B 22 (2004) 2811–2817.
[47] O. Auciello, J. Birrell, J. Carlisle, J. Gerbi, X. Xiao, B. Peng, H. Espinosa, Materials science and fabrication processes for a new MEMS technology based on ultrananocrystalline diamond thin films, Journal of Physics: Condensed Matter 16 (2004) R539–R552.
[48] X. Xiao, B.W. Sheldon, Y. Qi, A.K. Kothari, Intrinsic stress evolution in nanocrystalline diamond thin films with deposition temperature, Applied Physics Letters 92 (2008) 1–3, 131908.
[49] H.D. Espinosa, B.C. Prorok, B. Peng, K.H. Kim, N. Moldovan, O. Auciello, J.A. Carlisle, D.M. Gruen, D.C. Mancini, Mechanical properties of ultrananocrystalline diamond thin films relevant to MEMS/NEMS devices, Experimental Mechanics 43 (2003) 256–268.
[50] J.M. Lackner, W. Waldhauser, R. Ebner, M. Beutl, G. Jakopic, G. Leising, H. Hutter, M. Rosner, Pulsed laser deposition of non-stoichiometric silicon nitride (SiN_x) thin films, Applied Physics A 79 (2004) 1525–1527.
[51] H. Sato, A. Izumi, A. Masuda, H. Matsumura, Low-k silicon nitride film for copper interconnects process prepared by catalytic chemical vapour deposition method at low temperature, Thin Solid Films 395 (2001) 280–283.
[52] S.B. Patil, A. Kumbhar, P. Waghmare, V. Ramgopal Rao, R. Dusane, Low temperature silicon nitride deposited by Cat-CVD for deep sub-micron metal–oxide–semiconductor devices, Thin Solid Films 395 (2001) 270–274.
[53] S. Garcia, J. Martin, I. Martil, M. Fernandez, G. Gonzalez-Diaz, Deposition of low temperature Si-based insulators by the electron cyclotron resonance plasma method, Thin Solid Films 317 (1998) 116–119.
[54] A.J. Flewitt, A.P. Dyson, J. Robertson, W.I. Milne, Low temperature growth of silicon nitride by electron cyclotron resonance plasma enhanced chemical vapour deposition, Thin Solid Films 383 (2001) 172–177.
[55] F.S. Pool, Nitrogen plasma instabilities and the growth of silicon nitride by electron cyclotron resonance microwave plasma chemical vapour deposition, Journal of Applied Physics 81 (1997) 2839–2846.
[56] G.I. Isai, J. Holleman, H. Wallinga, P.H. Woerlee, Low hydrogen content silicon nitride films deposited at room temperature with an ECR plasma source, Journal of the Electrochemical Society 151 (2004) C649–C654.
[57] S. Jatta, K. Haberle, A. Klein, R. Schafranek, B. Koegel, P. Meissner, Deposition of dielectric films with inductively coupled plasma-CVD in dependence on pressure and two RF-Power-Sources, Plasma Processes and Polymers 6 (2009) S582–S587.
[58] L. Da Silva Zambom, R. Domingues Mansano, R. Furlan, Silicon nitride deposited by inductively coupled plasma using silane and nitrogen, Vacuum 65 (2002) 213–220.
[59] Q. Xu, Y. Ra, M. Bachman, G.P. Li, Characterization of low-temperature silicon nitride films produced by inductively coupled plasma chemical vapour deposition, Journal of Vacuum Science and Technology A 27 (2009) 145–156.
[60] A. Kshirsagar, P. Nyaupane, D. Bodas, S.P. Duttagupta, S.A. Gangal, Deposition and characterization of low temperature silicon nitride films deposited by inductively coupled plasma CVD, Applied Surface Science 257 (2011) 5052–5058.
[61] T. Owain, White paper—Inductively coupled plasma chemical vapour deposition (ICP-CVD), Oxford Instruments Plasma Technology Ltd, 2010.
[62] H. Zhou, K. Elgaid, C. Wilkinson, I. Thayne, Low-hydrogen-content silicon nitride deposited at room temperature by inductively coupled plasma deposition, Japanese Journal of Applied Physics 45 (2006) 8388–8392.
[63] S.S. Han, B.H. Jun, K. No, B.S. Bae, Preparation of a-SiN_x thin film with low hydrogen content by inductively coupled plasma enhanced chemical vapour deposition, Journal of the Electrochemical Society 145 (1998) 652–658.
[64] E. Dehan, P. Temple-Boyer, R. Henda, J.J. Pedroviejo, E. Scheid, Optical and structural properties of SiO_x and SiN_x materials, Thin Solid Films 266 (1995) 14–19.
[65] A.J. Bard, L.R. Faulkner, Electrochemical Methods: Fundamentals and Applications, 2nd Revised edition, John Wiley and Sons (WIE), New York, 2001.
[66] C. Gabrielli, M. Keddam, N. Portail, P. Rousseau, H. Takenouti, V. Vivier, Electrochemical impedance spectroscopy investigations of a microelectrode behavior in a thin layer cell: experimental and theoretical studies, Journal of Physical Chemistry 110 (2006) 20478–20485.

Biographies

E. Vanhove graduated in Science and Executive Engineering from the MINES Paris Tech (Ecole des Mines de Paris) in 2006. She joined the CEA (French Alternative Energies and Atomic Energy Commission, Paris, France) lab in 2006 and received a PhD in Materials Science in 2009 from the same school. In 2010, she rejoined the LAAS CNRS laboratory in Toulouse, France as a post-doctoral fellow. Her research interests are focused on the design, modelling, simulation, microfabrication and characterization of integrated electrochemical microsensors.

A. Tsopéla was born in Athens, Greece in 1988. She received the master degree in Chemical Engineering from the National Technical University of Athens (NTUA), in 2011. She joined the "Laboratoire d'Architecture et d'Analyse des Systèmes" of the "Centre National de la Recherche Scientifique" (LAAS-CNRS), in 2011 as PhD Student. She is carrying out her experimental research in the development of microsensors with environmental applications.

L. Bouscayrol was born in 1965. He worked at MOTOROLA Toulouse as an engineer for 14 years and obtained his "Physical Measurement" degree of technology from the Toulouse University (France), in 1993. In 2002, he joined the "Laboratoire d'Architecture et d'Analyse des Systèmes" of the "Centre National de la Recherche Scientifique" (LAAS-CNRS) in the "Techniques and Equipments Applied to Microelectronics" (TEAM) Service (TEAM) as an engineer. He is working on the development of thermal processes.

A. Desmoulin was born on 8th of March 1991 in Marseille. He received his "Physical Measurement" degree of technology from the Toulouse University (France), in 2011. In 2012, he obtained his professional license of "Instrumentation and Test in Complex Environment". In September 2012, he joined the "Laboratoire d'Architecture et d'Analyse des Systèmes" of the "Centre National de la Recherche Scientifique" (LAAS-CNRS) in the "Techniques and Equipments Applied to Microelectronics" (TEAM) Service (TEAM) as an engineer. He is working on the development of thermal processes technologies.

J. Launay was born on the 11th of March 1975. He received the degree in electronic engineering from the Institut National des Sciences Appliquées de Toulouse (France) in 1998. He joined the "Laboratoire d'Architecture et d'Analyse des Systèmes" of the "Centre National de la Recherche Scientifique" (LAAS-CNRS) in 1998 and received the PhD degree from the Institut National des Sciences Appliquées de Toulouse (France) in 2001. In 2002, he became lecturer at the Université Paul Sabatier de Toulouse (France). His research activities include the development of chemical microsensors for the detection in liquid phase.

P. Temple-Boyer was born on October 25, 1966. He received his Engineer Master's Degree in electronic engineering from the Ecole Supérieure d'Electricité (Paris, France) in 1990 and his Master's Degree in microelectronics from the Université Paul Sabatier de Toulouse (France) in 1992. He joined the "Laboratoire d'Architecture et d'Analyse des Systèmes" of the "Centre National de la Recherche Scientifique" (LAAS-CNRS) in 1992 and received the PhD degree from the Institut National des Sciences Appliquées de Toulouse (France) in 1995. Since then, as a senior researcher, he has been working on the development of micro- and nanotechnologies.